Progress In Electromagnetics Research M, Vol. 105, 161–172, 2021

Sensorless Control of Permanent Magnet Synchronous Motor Based on T-S Fuzzy Inference Algorithm Fractional Order Sliding Mode

Yilin Zhu*, Yang Bai, Hao Wang, and Lei Sun

Abstract—In order to improve the robustness of the fractional order sliding mode controller (FSMC) for permanent magnet synchronous motor (PMSM) sensorless control, a fractional order sliding mode controller based on T-S fuzzy inference algorithm (FFSMC) is proposed to observe the rotor speed and position information. Based on the mathematical model of PMSM and sliding mode controller, a fractional order sliding mode controller is designed, and its stability is proved. The T-S fuzzy inference algorithm is used to tune the reaching law parameters of the FSMC, so that the reaching law parameters are no longer fixed values, but change with the state of the system. The correctness of the proposed method is verified by MATLAB simulation software. The effectiveness of the simulation results is verified by building a PMSM sensorless control experimental platform. The results show that the PMSM sensorless control based on FFSMC achieves parameter self-tuning and improves the observation accuracy. And the robustness of the control system is enhanced.

1. INTRODUCTION

Compared with other types of motors, permanent magnet synchronous motor (PMSM) excitation field is provided by permanent magnets, and the rotor does not require excitation current. It has the advantages of high efficiency, high power density, high efficiency, and small size. It is widely used in aerospace, semiconductor industry, national defense industry, and other industrial fields [1, 2]. Regarding PMSM control, whether it is vector control or direct control, the rotor position information and speed information of the motor need to be collected during the control process. In actual control systems, rotor position information is generally collected by mechanical sensors. This method not only increases the cost of the control system, but also causes the problem of reduced detection accuracy due to long term exposure of mechanical sensors to harsh environments. Therefore, it is necessary to study the sensorless control of PMSM [3].

The principle of sensorless technology is to measure the voltage and current signals related to the rotor position information, and then calculate the rotor position and speed through the estimation algorithm. At present, there are mainly two methods: 1) the method based on the mathematical model and 2) the algorithm based on the salient pole model. The specific methods are: back-EMF estimation method, high frequency injection method [4], model reference adaptive algorithm [5], extended Kalman filter algorithm [6], and sliding mode controller (SMC). Among them, SMC has the advantages of small dependence on motor parameters and strong robustness, and is widely used in sensorless control of PMSM. However, the inherent chattering problem of SMC will increase the energy consumption of the system and affect the estimation accuracy [7].

In [8], an improved SMC is designed, using the sigmoid function instead of the traditional sgn function to solve the rotor chattering problem, but there is a problem of complex calculations. In [9], a new SMO is proposed to estimate the rotor position and speed, using the S-shaped switching function

Received 25 July 2021, Accepted 22 October 2021, Scheduled 4 November 2021
* Corresponding author: Yilin Zhu (yl.zhu.dy@gmail.com).
The authors are with the Jiangsu Changjiang Intelligent Manufacturing Research Institute Co, Ltd, Changzhou 213001, China.

to improve the sign function to estimate the back electromotive force (EMF). However, the above two methods of improving the sgn function will weaken the robustness of the system. A sliding mode controller based on active flux is proposed to estimate rotor position and speed [10–11]. Although this method is suitable for control systems with different speed ranges, it is more sensitive to system parameter changes.

Therefore, a fractional order sliding mode controller (FSMC) is proposed, with energy transfer slower than conventional calculus [12]. By introducing a fractional order reaching law, the chattering caused by general sliding mode control is weakened. In [13], saturation function is used to weaken the chattering of the FSMC. The fractional order phase-locked loop is used to extract the rotor speed and rotor position. In addition, the FSMC can also be combined with an extended Kalman filter to realize sensorless control of PMSM [14]. Due to the use of a large number of parameters, the observation accuracy can be greatly improved.

As we all know, the choice of the reaching law coefficient also has a great influence on the jitter amplitude value of the FSMC. In order to meet the nonlinearity, real-time performance and anti-interference performance of the control system, the reaching law coefficient cannot be set as a fixed value, but needs to be adjusted according to the state of the system. In [15], the fuzzy control algorithm is introduced into SMC. This method does not need to design a precise control rate, but the control accuracy is not high. In [16], a fuzzy neural network is used to optimize the control gain of the FSMC. However, the neural network requires a lot of training, which will increase the calculation time. The first order T-S fuzzy inference algorithm not only saves the steps of fuzzification and simplifies the calculation process, but can also generate more complex nonlinear functions with a small number of fuzzy rules. It can effectively reduce the number of fuzzy rules when dealing with multivariable nonlinear systems, which has great advantages [17].

In this paper, the first order T-S fuzzy algorithm is used to tune the reaching law parameters of the FSMC to form a PMSM sensorless control system based on FFSMC. Matlab simulation software is used to verify the effectiveness of the control strategy proposed in this paper. In addition, a PMSM sensorless control experiment platform was built to verify the simulation results.

2. MATHEMATICAL MODELS OF THE PMSM AND SMC

2.1. Mathematical Model of the PMSM

The stator winding of the PMSM is identical to the ordinary synchronous motor, while the excitation winding in the rotor is replaced with the permanent magnet, so the mathematical model of PMSM is similar to the mathematical model of ordinary synchronous motor. Under the premise of satisfying accuracy, the following assumptions are often made [18]:

1) Ignoring the magnetic resistance of stator and rotor core.
2) Ignoring the magnetic path saturation.
3) Ignoring the effects of damping windings and high harmonics.
4) Ignoring the hysteresis and vortex losses.

In the d-q axis, the voltage and flux linkage of the PMSM are:

$$\begin{aligned} \begin{bmatrix} u_{\mathrm{d}} \\ u_{\mathrm{q}} \end{bmatrix} &= \begin{bmatrix} R + L_{\mathrm{q}} \cdot p & -\omega_e L_{\mathrm{q}} \\ \omega_e L_{\mathrm{d}} & R + L_{\mathrm{q}} \cdot p \end{bmatrix} \begin{bmatrix} i_{\mathrm{d}} \\ i_{\mathrm{q}} \end{bmatrix} + \omega_e \psi_f \begin{bmatrix} 0 \\ 1 \end{bmatrix} \\ \psi_{\mathrm{d}} &= L_{\mathrm{d}} i_{\mathrm{d}} + \psi_f \\ \psi_{\mathrm{q}} &= L_{\mathrm{q}} i_{\mathrm{q}} \end{aligned} \tag{1}$$

where u_{d} and u_{q} are stator voltages in d- and q-axes, respectively; i_{d} and i_{q} are stator currents in d- and q-axes, respectively; L_{d} and L_{q} are inductance in d- and q-axes, respectively; R is the resistance of windings; ω_e is the rotor electrical angular velocity; p is the number of pole pairs; ψ_{d} and ψ_{q} are stator flux linkages in d- and q-axes, respectively; ψ_f is the flux linkage of permanent magnet.

The voltage equation for the PMSM under the α-β axis is:

$$\begin{cases} u_\alpha = (R + pL_{\mathrm{d}}) i_\alpha + [\omega_e (L_{\mathrm{d}} - L_{\mathrm{q}})] i_\beta + E_\alpha \\ u_\beta = [-\omega_e (L_{\mathrm{d}} - L_{\mathrm{q}})] i_\alpha + (R + pL_{\mathrm{d}}) i_\beta + E_\beta \end{cases} \tag{2}$$

where u_α and u_β are stator voltages in α- and β-axes, respectively; i_α and i_β are stator currents in α- and β-axes, respectively; E_α and E_β are expansion of the back-EMF in α- and β-axes, respectively.

The surface mounted permanent magnet synchronous motor is the research object of this paper, and the components of the stator inductance on the d-q axis are equal ($L_\mathrm{d} = L_\mathrm{q}$). Therefore, the voltage equation can be simplified to:

$$\begin{cases} u_\alpha = (R + pL_\mathrm{d})i_\alpha + E_\alpha \\ u_\beta = (R + pL_\mathrm{d})i_\beta + E_\beta \end{cases} \tag{3}$$

The state equation of the PMSM that can be derived by Equation (3) is:

$$\begin{cases} \dfrac{\mathrm{d}i_\alpha}{\mathrm{d}t} = -\dfrac{R}{L_\mathrm{d}}\, i_\alpha + E_\alpha + \frac{1}{L_\mathrm{d}}\, u_\alpha \\ \dfrac{\mathrm{d}i_\beta}{\mathrm{d}t} = -\dfrac{R}{L_\mathrm{d}}\, i_\beta + E_\beta + \frac{1}{L_\mathrm{d}}\, u_\beta \\ \dfrac{\mathrm{d}\psi_\alpha}{\mathrm{d}t} = -Ri_\alpha + u_\alpha \\ \dfrac{\mathrm{d}\psi_\beta}{\mathrm{d}t} = -Ri_\beta + u_\beta \end{cases} \tag{4}$$

where ψ_α and ψ_β are stator flux linkages in α- and β-axes, respectively.

2.2. Mathematical Models of the Traditional Sliding Mode Controller

The basic principle of using the traditional sliding mode controller (TSMC) to realize the sensorless control of PMSM is:

1) After detecting the voltage and current of the motor stator, using the observation error of the stator current to design the sliding mode surface.
2) Taking the back EMF when the system reaches the sliding mode surface Observed value.
3) Calculating the rotor position and speed through the observed value of back electromotive force.

As shown in Figure 1.

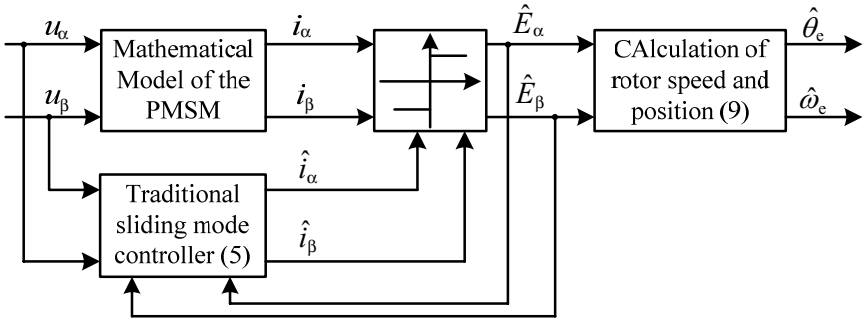

Figure 1. Block diagram of the traditional sliding mode controller structure.

In the literature, the sliding surface is designed as:

$$S(x) = \hat{i} - i \tag{5}$$

where $i = [\ i_\alpha \quad i_\beta\ ]$ is the measured value of the stator current, $\hat{i} = [\ \hat{i}_\alpha \quad \hat{i}_\beta\ ]$ is the estimated value of the current.

The TSMC can be constructed from the state equation of PMSM as follows:

$$\begin{cases} \dfrac{\mathrm{d}\hat{i}_\alpha}{\mathrm{d}t} = -\dfrac{R}{L_\mathrm{d}}\, \hat{i}_\alpha - \dfrac{1}{L_\mathrm{d}}\, k\,\mathrm{sgn}\left(\hat{i}_\alpha - i_\alpha\right) + \dfrac{1}{L_\mathrm{d}}\, u_\alpha \\ \dfrac{\mathrm{d}\hat{i}_\beta}{\mathrm{d}t} = -\dfrac{R}{L_\mathrm{d}}\, \hat{i}_\beta - \dfrac{1}{L_\mathrm{d}}\, k\,\mathrm{sgn}\left(\hat{i}_\beta - i_\beta\right) + \dfrac{1}{L_\mathrm{d}}\, u_\beta \end{cases} \tag{6}$$

where k is the switching gain, and sgn is the sign function.

It can be derived by subtracting formula (4) from formula (6):

$$\begin{cases} \dfrac{\mathrm{d}(\hat{i}_\alpha - i_\alpha)}{\mathrm{d}t} = -\dfrac{R}{L_\mathrm{d}}\left(\hat{i}_\alpha - i_\alpha\right) - \dfrac{1}{L_\mathrm{d}}\, k\,\mathrm{sgn}(\hat{i}_\alpha - i_\alpha) + \dfrac{1}{L_\mathrm{d}}\, E_\alpha \\ \dfrac{\mathrm{d}(\hat{i}_\beta - i_\beta)}{\mathrm{d}t} = -\dfrac{R}{L_\mathrm{d}}(\hat{i}_\beta - i_\beta) - \dfrac{1}{L_\mathrm{d}}\, k\,\mathrm{sgn}(\hat{i}_\beta - i_\beta) + \dfrac{1}{L_\mathrm{d}}\, E_\beta \end{cases} \tag{7}$$

According to the basic principle of the TSMC to realize the PMSM sensorless control, when the sliding mode surface is reached, the expression of the back-EMF can be derived as:

$$\begin{cases} E_\alpha = k\,\mathrm{sgn}\left(\hat{i}_\alpha - i_\alpha\right) \\ E_\beta = k\,\mathrm{sgn}\left(\hat{i}_\beta - i_\beta\right) \end{cases} \tag{8}$$

$$\begin{cases} E_\alpha = -\psi_f\,\omega_e \sin\theta_e \\ E_\beta = \psi_f\,\omega_e \cos\theta_e \end{cases} \tag{9}$$

It can be seen from the above formula that the speed and position information of the PMSM can be obtained from the back-EMF E_α and E_β, as shown in formula (10):

$$\begin{cases} \hat{\theta}_\mathrm{e} = \arctan\left(-\dfrac{\hat{E}_\alpha}{\hat{E}_\beta}\right) \\ \hat{\omega}_\mathrm{e} = \dfrac{\mathrm{d}\hat{\theta}_\mathrm{e}}{\mathrm{d}t} \end{cases} \tag{10}$$

where $\hat{E}_\alpha$, $\hat{E}_\beta$ is the estimated value of back-EMF.

3. DESIGN OF SENSORLESS CONTROLLER OF PMSM

3.1. Design of Fractional Order Sliding Mode Controller

Compared with the TSMC, fractional order sliding mode controller (FSMC) uses the slow and convergent characteristics of the energy transfer of a fractional order system to reduce the switching frequency and switching speed of the system state variables on the sliding mode surface, so that the convergence speed is faster and smoother, which can effectively improve the robustness of the system. And it is conducive to the stable control of PMSM. Before designing a fractional sliding mode controller, considering that the inductance and capacitance of the motor have the characteristics of fractional order, they need to be processed. The motor's motion equation and voltage equation can be obtained after Laplace transform:

$$\begin{cases} \dfrac{I(s)}{U(s) - E(s)} = \dfrac{1}{L_\mathrm{d} s + R} \\ \dfrac{E(s)}{I(s) - I_f(s)} = \dfrac{K_M C_e}{J s + B_m} \end{cases} \tag{11}$$

where J is the moment of inertia, B_m the viscous friction coefficient, K_M the torque coefficient, C_e the back electromotive force constant, and I_f the load current.

Furthermore, by extending the motion equation and voltage equation of PMSM to the fractional order, and performing Laplace transform on it:

$$\begin{cases} u = Ri + L_\mathrm{d} \times {}_0D_t^\lambda i + E \\ {}_0D_t^\sigma \omega_\mathrm{e} = -\dfrac{B_m}{J}\omega_\mathrm{e} + \dfrac{K_M}{J} i - \frac{1}{J} T \end{cases} \quad \Rightarrow \quad \begin{cases} \dfrac{I(s)}{U(s) - E(s)} = \dfrac{1}{L_\mathrm{d} s^\lambda + R} \\ \dfrac{E(s)}{I(s) - I_f(s)} = \dfrac{K_M C_e}{J s^\sigma + B_m} \end{cases} \tag{12}$$

where ${}_0D_t^\lambda$ is the fractional order calculus operator.

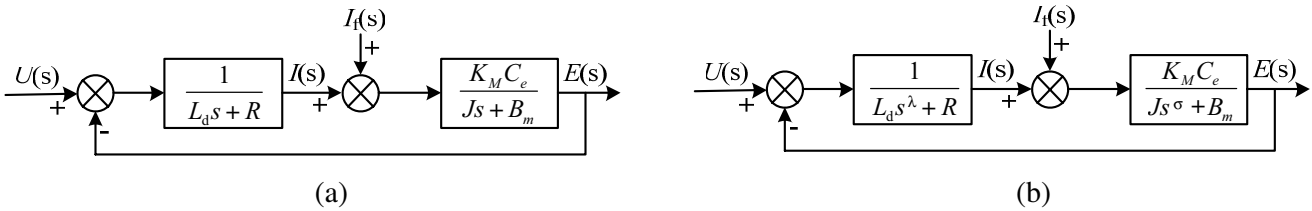

Figure 2. The equivalent structure block diagram of PMSM. (a) Traditional. (b) Fractional order.

The Laplace transform results obtained from Equations (11) and (12) are drawn in the form of a structural block diagram, as shown in Figure 2.

Decomposing the fractional voltage in Equation (12) on the α-β axis:

$$\begin{bmatrix} u_\alpha \\ u_\beta \end{bmatrix} = R \begin{bmatrix} i_\alpha \\ i_\beta \end{bmatrix} + L_{\mathrm{d}} \times {}_0D_t^\lambda \times \begin{bmatrix} i_\alpha \\ i_\beta \end{bmatrix} + \begin{bmatrix} E_\alpha \\ E_\beta \end{bmatrix} \tag{13}$$

Construct the dynamic equation by formula (13):

$$\begin{bmatrix} u_\alpha \\ u_\beta \end{bmatrix} = R \begin{bmatrix} \hat{i}_\alpha \\ \hat{i}_\beta \end{bmatrix} + L_{\mathrm{d}} \times {}_0D_t^\lambda \times \begin{bmatrix} \hat{i}_\alpha \\ \hat{i}_\beta \end{bmatrix} + \begin{bmatrix} \hat{E}_\alpha \\ \hat{E}_\beta \end{bmatrix} \tag{14}$$

Subtracting Equation (14) from Equation (13), the current observation error is:

$${}_0D_t^\lambda \begin{bmatrix} u_\alpha \\ u_\beta \end{bmatrix} = -\frac{R}{L_{\mathrm{d}}} \begin{bmatrix} \tilde{i}_\alpha \\ \tilde{i}_\beta \end{bmatrix} + \frac{1}{L_{\mathrm{d}}} \begin{bmatrix} \tilde{E}_\alpha \\ \tilde{E}_\beta \end{bmatrix} \tag{15}$$

where $\tilde{i}_\alpha = \hat{i}_\alpha - i_\alpha$, $\tilde{i}_\beta = \hat{i}_\beta - i_\beta$ is the current error, and $\tilde{E}_\alpha = \hat{E}_\alpha - E_\alpha$, $\tilde{E}_\beta = \hat{E}_\beta - E_\beta$ is the back-EMF error.

The fractional sliding mode surface is design as:

$$S^{\mathrm{a}} = \tilde{i} + \lambda_0 \times {}_0D_t^b \tag{16}$$

where $\tilde{i} = \begin{bmatrix} \tilde{i}_\alpha & \tilde{i}_\beta \end{bmatrix}^T$.

Find the derivative of the above formula:

$${}_0D_t^\lambda s = {}_0D_t^\lambda \tilde{i} + c \times {}_0D_t^{b+\lambda} \tilde{i} = \frac{1}{L_{\mathrm{d}}} \left(-R\tilde{i} + E - \hat{E} \right) + c \times {}_0D_t^{b+\lambda} \tilde{i} \tag{17}$$

where $\tilde{E} = \begin{bmatrix} \tilde{E}_\alpha & \tilde{E}_\beta \end{bmatrix}^T$, c is the coefficient.

The choice of the reaching law is very important to the control performance of the sliding mode controller, and it represents the way that the system reaches the sliding mode surface. The fractional exponential reaching law chosen in this paper is:

$${}_0D_t^\lambda S = -\mu s - \varepsilon \mathrm{sgn}(s) \tag{18}$$

where μ, ε is the coefficient of the reaching law, and $\mu > 0$, $\varepsilon > 0$.

In summary, the calculation formula for the estimated value of back-EMF can be derived as:

$$\hat{E} = -Ri + L_{\mathrm{d}} \times c \times {}_0D_t^{b+\lambda} \tilde{i} + \mu s + \varepsilon \mathrm{sgn}(s) \tag{19}$$

After obtaining the estimated value of the back-EMF, the speed and position information of the PMSM can be obtained by formula (10). The structural block diagram of the designed FSMC is shown in Figure 3.

After completing the above design steps, it is necessary to conduct stability analysis of the designed sliding mode controller. Take the Lyapunov function: $V(t) = \frac{1}{2} S^T S$, and find the fractional derivative of it:

$${}_0D_t^\lambda V \leq S \times_0 D_t^\lambda S = S \left[\frac{1}{L_{\mathrm{d}}} \left(-R\tilde{i} + E - \hat{E} \right) + c \times {}_0D_t^{b+\lambda} \tilde{i} \right] \tag{20}$$

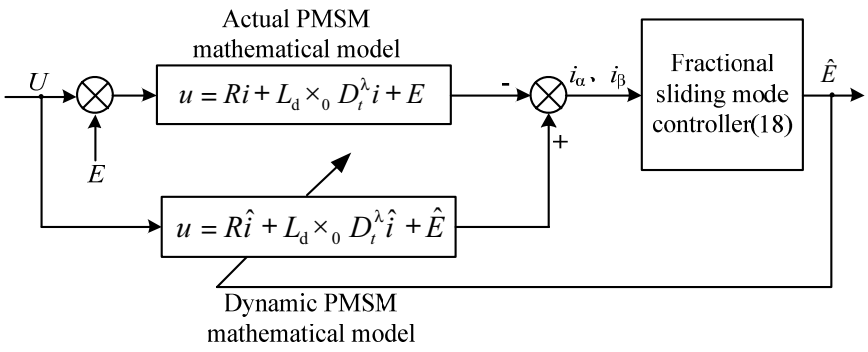

Figure 3. Structure block diagram of the fractional order sliding module controller.

Simplifying Equation (20) can be obtained:

$$ {}_0D_t^\lambda V \le S\left[-\mu s - \varepsilon \mathrm{sgn}(s) + \frac{1}{L_\mathrm{d}}E\right] \le -\mu S^2 - \left(\varepsilon - \frac{1}{L_\mathrm{d}}E\right)|S| \tag{21} $$

It can be seen from formula (21) that when $-\varepsilon > \frac{1}{L_d}|E|$ and $\mu > 0$ are satisfied at the same time, $V(t) < 0$ can be obtained, which satisfies the system stability condition.

3.2. Design of Fuzzy Fractional Order Sliding Mode Controller

It can be seen from the analysis in Section 3.1 that the magnitude of the approach rate parameter ε has a greater impact on the chattering amplitude value of the sliding mode controller. In the control system, when the controller error is large, the ε value needs to be increased. On the contrary, the ε value needs to be decreased. Therefore, in order to meet nonlinearity, real time performance, and anti-interference performance of the system, ε cannot be set as a fixed value, but needs to be adjusted according to the system state. This paper proposes to use the first order T-S fuzzy inference algorithm to set the value of ε. The fuzzy control system takes the sliding mode surface S and its derivative dS as the input, and the absolute value of the output Δu as the reaching law parameter ε. The structure diagram of the first order T-S fuzzy inference algorithm is shown in Figure 4.

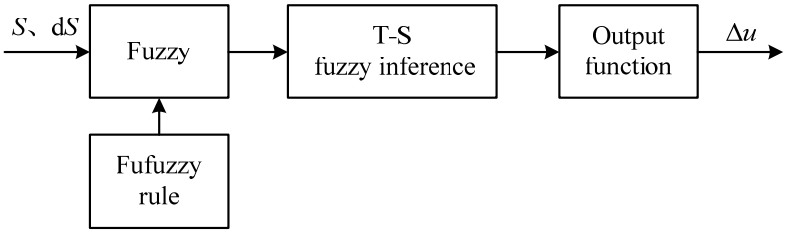

Figure 4. Structure block diagram of T-S fuzzy inference.

Table 1. Fuzzy control rules.

S / $\mathrm{d}S$	n	z	p	n	z	p	n	z	p
s	s	s	m	s	s	m	s	s	m
m	s	m	l	s	m	l	s	m	l
l	m	l	l	m	l	l	m	l	l

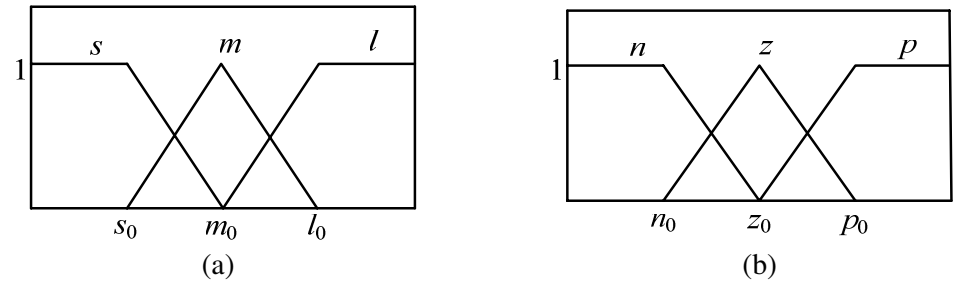

Figure 5. Membership function. (a) Sliding mode surface S; (b) Sliding mode surface derivative dS.

The sliding mode surface S is divided into three fuzzy sets: s (small), m (medium), and l (large). Similarly, the sliding mode surface derivative d_S is also divided into three fuzzy sets: n (negative), z (zero), and p (positive), and use triangular membership functions to achieve fuzzification, as shown in Figure 5. Table 1 lists the fuzzy rules.

In addition, the output of the system is also divided into three levels: s (small), m (medium), and l (large). The fuzzy subset membership function expressions of input S and dS are:

$$\xi_S = \begin{cases} \xi_s(x) = \begin{cases} 1 & x < s_0 \\ \dfrac{m_0 - x}{m_0 - s_0} & s_0 \le x \le m_0 \end{cases} \\ \xi_m(x) = \begin{cases} \dfrac{x - s_0}{m_0 - s_0} & s_0 \le x \le m_0 \\ \dfrac{l_0 - x}{l_0 - m_0} & m_0 < x \le l_0 \end{cases} \\ \xi_l(x) = \begin{cases} \dfrac{x - m_0}{l_0 - m_0} & m_0 < x \le l_0 \\ 1 & x > l_0 \end{cases} \end{cases} \tag{22}$$

$$\xi_{\mathrm{d}S} = \begin{cases} \xi_n(x) = \begin{cases} 1 & x < n_0 \\ \dfrac{z_0 - x}{z_0 - n_0} & n_0 \le x \le z_0 \end{cases} \\ \xi_z(x) = \begin{cases} \dfrac{x - n_0}{z_0 - n_0} & n_0 \le x \le z_0 \\ \dfrac{p_0 - x}{p_0 - z_0} & z_0 < x \le p_0 \end{cases} \\ \xi_p(x) = \begin{cases} \dfrac{x - z_0}{p_0 - z_0} & z_0 < x \le p_0 \\ 1 & x > p_0 \end{cases} \end{cases} \tag{23}$$

After tuning the reaching law parameters by TS fuzzy inference algorithm, a fuzzy fractional order sliding mode controller (FFSMC) is designed, which can be used in the sensorless control system of PMSM. The sensorless control of PMSM based on FFSMC can effectively reduce the chattering amplitude value which improves the robustness of the control system.

3.3. Sensorless Control Based on FFSMC of PMSM

The block diagram of PMSM sensorless control system based on FFSMC is shown in Figure 6. The rotor speed and rotor position feedback are calculated by the FFSMC module, and a speed closed loop system is formed to control the PMSM rotor to rotate at a given speed. The estimated value of rotor speed $\hat{\omega}_e$ is calculated by the FFSMC module and compared with the given value ω of speed. The obtained speed error is adjusted by the PI controller, which realizes the closed loop control of speed by replacing the traditional speed sensor with the speed observer.

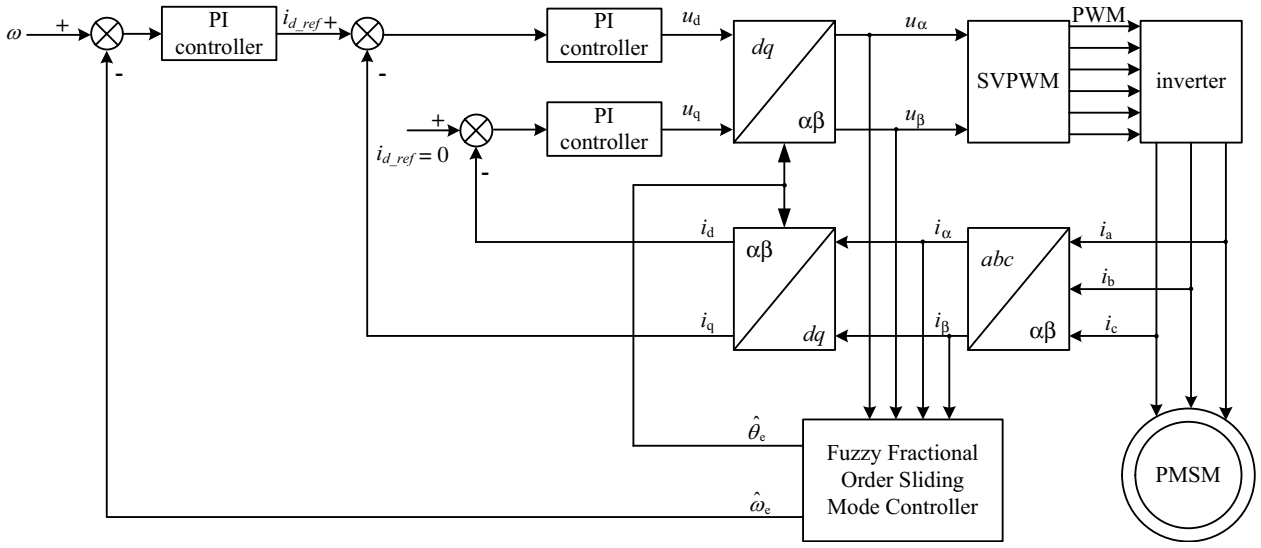

Figure 6. Structure block diagram of PMSM sensorless control system based on the FFSMC.

4. SIMULATION VERIFICATION

In order to verify the correctness and effectiveness of the FFSMC proposed in this paper to achieve PMSM sensorless control, the two control strategies of traditional SMC and FFSMC were compared and analyzed using Matlab/Simulink software. The simulation settings are: the given speed is 1000 r/min; the simulation time is 0.4 s. Focusing on the rotor position and its error, the rotor speed and its error have been analyzed.

Figure 7 and Figure 8 are the estimated values of rotor position and error of the traditional SMC and FFSMC, respectively. It can be seen that the rotor position estimation error of the traditional SMC is about 0.34 rad, while the rotor position estimation error of the FFSMC is only 0.07 rad. The rotor position error of the proposed FFSMC is reduced by 79.12%. Therefore, the rotor position observation accuracy of the proposed FFSMC is higher.

Figure 9 and Figure 10 show the estimated values of the rotational speed and rotational speed error of the traditional SMC and FFSMC, respectively. It can be seen from the figures that compared

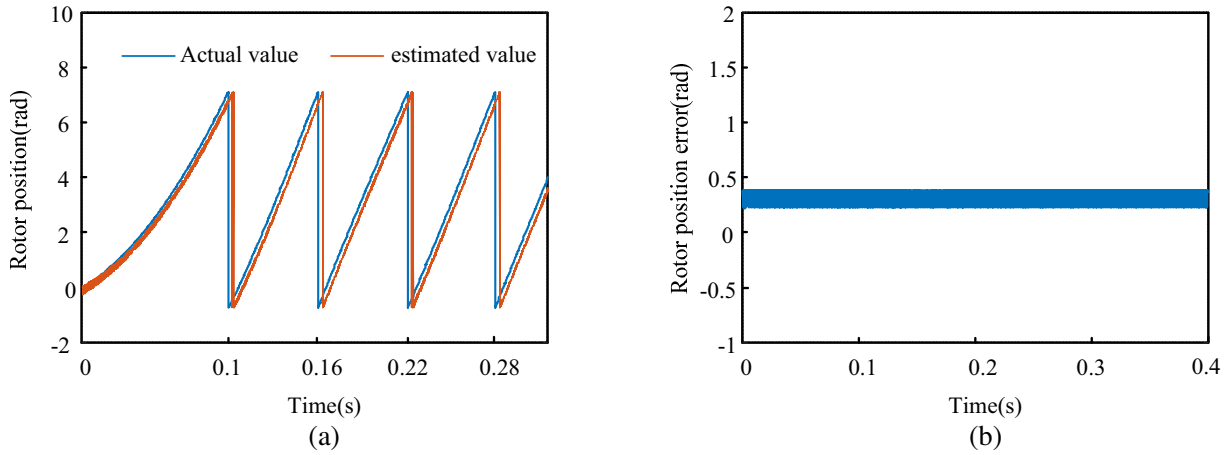

Figure 7. Rotor position observation of traditional SMC. (a) Rotor position estimate. (b) Rotor position estimate error.

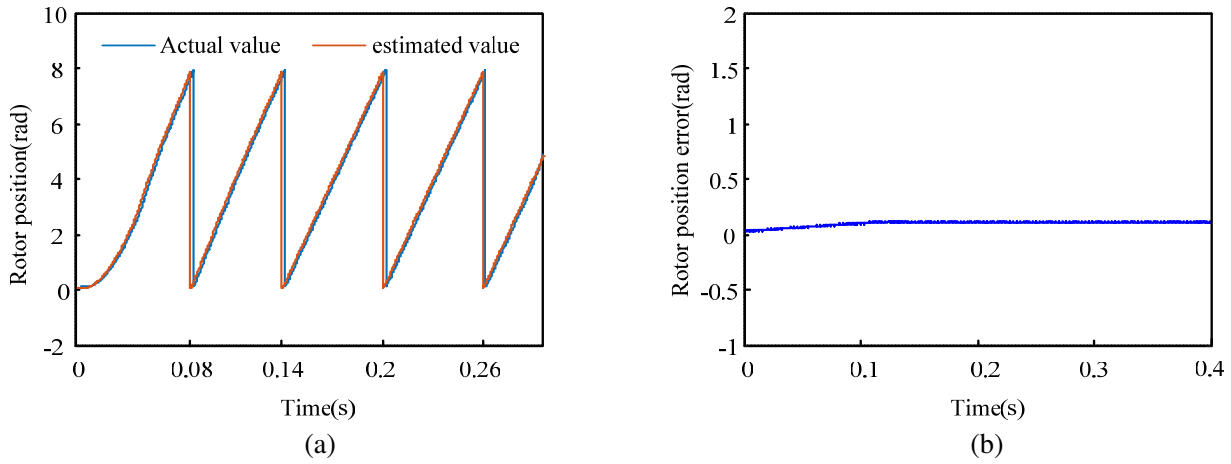

Figure 8. Rotor position observation of FFSMC. (a) Rotor position estimate. (b) Rotor position estimate error.

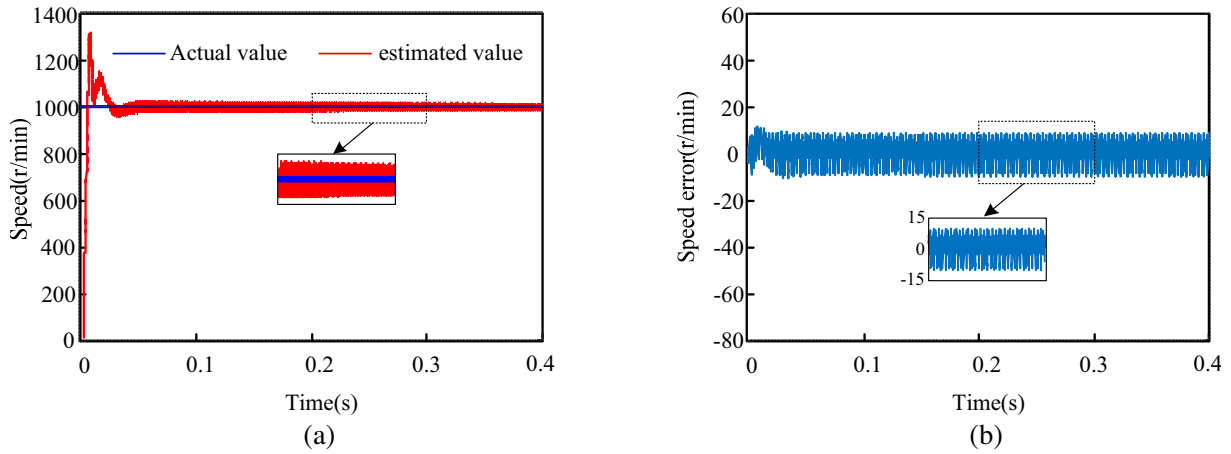

Figure 9. Rotor speed observation of traditional SMC. (a) Rotor speed estimate. (b) Rotor speed estimate error.

to a conventional controller, the speed response curve of FFSMC is smoother, and the error is smaller, which is only about ± 3 r/min. While the traditional SMC reached 10 r/min, indicating that the speed error decreased by about 70%. Therefore, the rotational speed observation accuracy of the proposed FFSMC is higher.

5. EXPERIMENTAL RESULTS

According to the above analysis, the PMSM sensorless control experimental platform based on FFSMC is built, as shown in Figure 11. The motor parameters are listed in Table 2.

In order to verify the effectiveness of the control strategy proposed in this paper, the experimental waveforms of the traditional SMC and FFSMC are presented. Figures 12 and 13 are waveform graphs of the motor speed, rotor position, and error of FFSMC and traditional SMC at no-load, respectively. It can be seen from Figure 13(b) that the rotor position error of traditional SMC is about 12°. From Figure 12(b), the rotor position error of FFSMC is about 6°, and the speed waveform is smoother. Figure 12 is an experimental waveform diagram. Hence, the speed and rotor position estimated by FFSMC ensure good accuracy and stability, and the speed fluctuation is small, which can effectively track and accurately estimate the rotor position and speed.

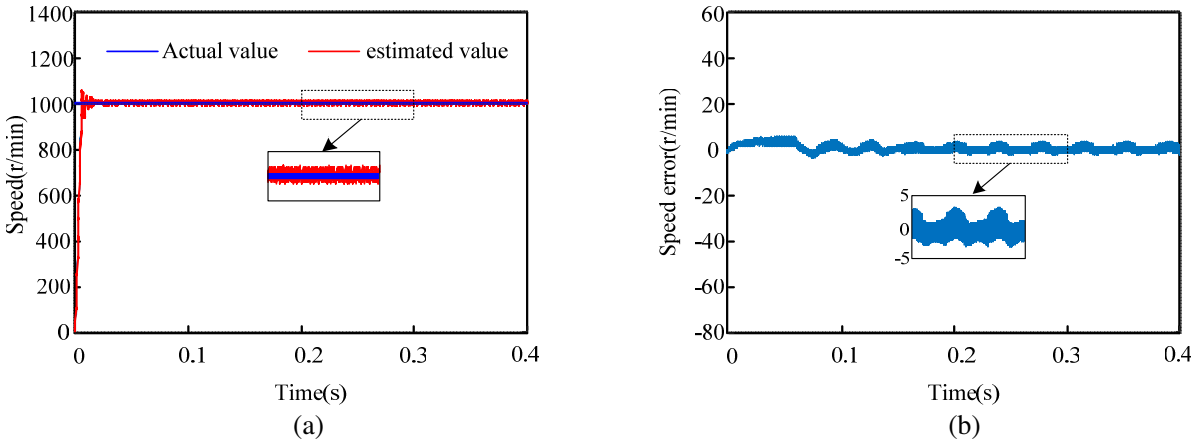

Figure 10. Rotor speed observation of FFSMC. (a) Rotor speed estimate. (b) Rotor speed estimate error.

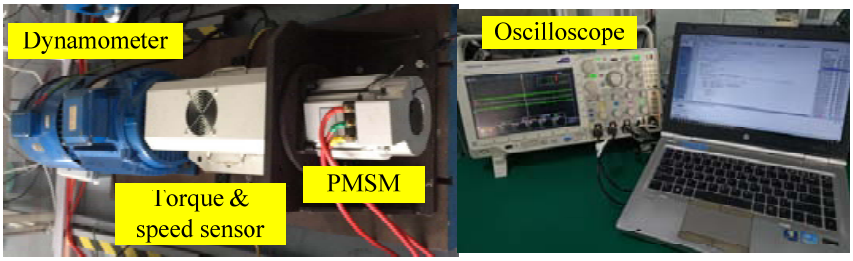

Figure 11. The experiment platform of PMSM sensorless control.

Table 2. Parameter of the motor.

Symbol	Value	Symbol	Value
P_n/W	20	n/(r/min)	3600
$U_{\rm dc}$/V	96	R/Ω	0.006
I_n/A	190	ψ_f/Wb	0.03
T_e/(N·m)	54	P	4
L/(cm)	108	Frequency (kHz)	16

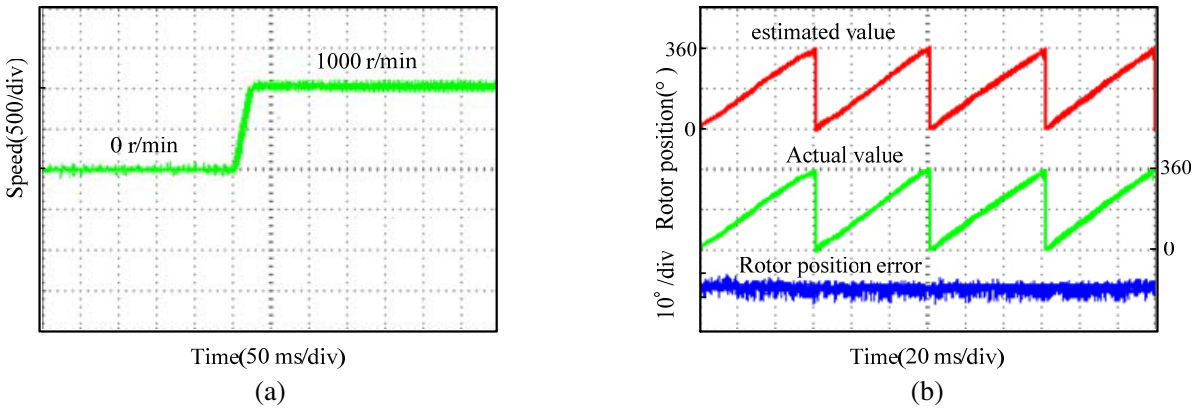

Figure 12. Experimental results of FFSMC. (a) Speed curve. (b) Rotor position.

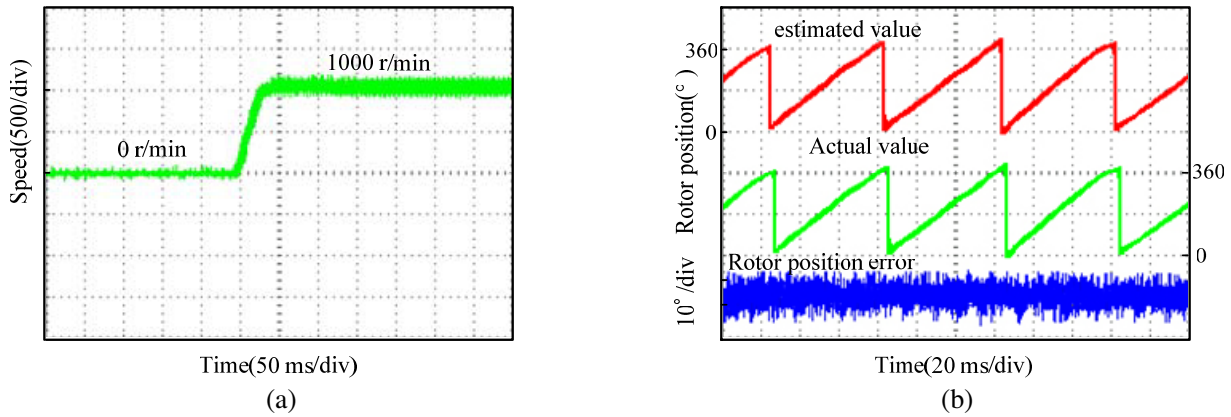

Figure 13. Experimental results of traditional SMC. (a) Speed curve. (b) Rotor position.

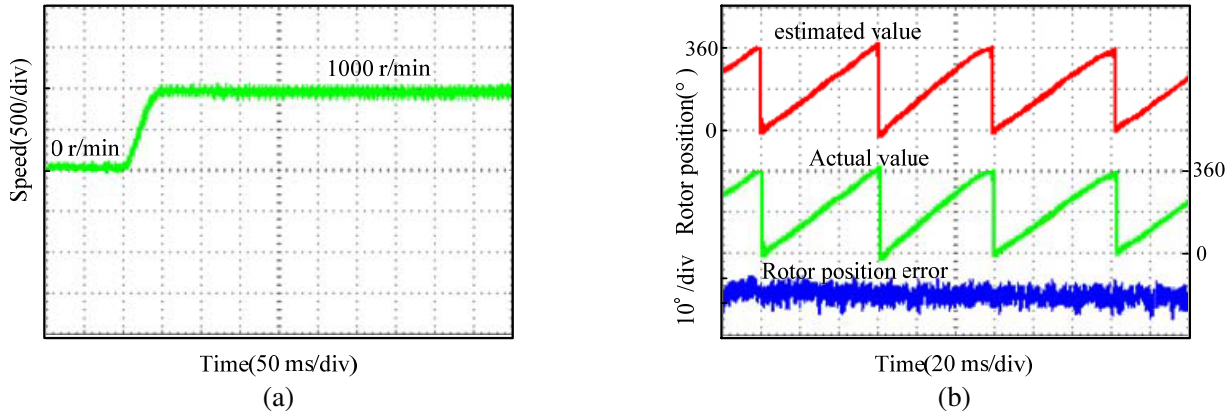

Figure 14. Experimental results of FFSMC under full-load condition. (a) Speed curve. (b) Rotor position.

Figure 14 shows the waveforms of the FFSMC result under full-load condition. As can be seen from it, the rotor position error when the motor is full load is about 8°, which increases by 2° more than when the motor is no-load. Although the rotor position error increased, it had better tracking performance. In conclusion, the control strategy proposed in this paper has good position estimation accuracy for both no-load and full load conditions.

6. CONCLUSION

In this paper, an FFSMC controller is used to estimate the rotor position and speed in the surface mounted PMSM sensorless control system. Combining the first-order T-S fuzzy algorithm with FSMO, the parameters in the reaching law of the FSMC are adjusted online to make them change with the state of the control system. The simulation and experiment results show that the FFSMC proposed in this paper not only reduces the chattering amplitude value of the traditional sliding mode control, but also improves the observation accuracy of the rotor position and speed. The proposed method is of great significance to the sensorless research of PMSM.

REFERENCES

1. Hu, Q., L. Ling, Z. Cheng, et al., "Researching for sensorless control of PMSM based on a novel sliding mode observer," *2018 3rd International Conference on Advanced Robotics and Mechatronics*, 542–547, 2018.

2. Pan, Y., X. Liu, Y. Zhu, B. Liu, and Z. Li, "Feedforward decoupling control of interior permanent magnet synchronous motor with genetic algorithm parameter identification," *Progress In Electromagnetics Research M*, Vol. 102, 117–126, 2021.
3. Sun, P., Q. Ge, B. Zhang, et al., "Sensorless control technique of PMSM based on RLS on-line parameter identification," *2018 21st International Conference on Electrical Machines and Systems*, 1670–1673, 2018.
4. Ni, R., K. Lu, F. Blaabjerg, et al., "A comparative study on pulse sinusoidal high frequency voltage injection and INFORM methods for PMSM position sensorless control," *2016 42nd Annual Conference of the IEEE Industrial Electronics Society*, 2600–2605, 2016.
5. He, Y., "Speed observation of high-speed permanent magnet synchronous motor based on fuzzy MRAS," *Chinese Control Conf. CCC*, Vol. 2020, 3550–3555, 2020.
6. Farhan, A., M. Abdelrahem, A. Saleh, et al., "Robust sensorless direct speed predictive control of synchronous reluctance motor," *IEEE Int. Symp. Ind. Electron.*, Vol. 2020, 1541–1546, June 2020.
7. Vieira, R. P., C. C. Gastaldini, R. Z. Azzolin, et al., "Sensorless sliding-mode rotor speed observer of induction machines based on magnetizing current estimation," *IEEE Trans. Ind. Electron.*, Vol. 61, No. 9, 4573–4582, 2014.
8. Yuan, Q., Y. Yang, H. Wu, et al., "Low speed sensorless control based on an improved sliding mode observation and the inverter nonlinearity compensation for SPMSM," *IEEE Access*, Vol. 8, 61299–61310, 2020.
9. Yahui, Z., F. Ming, and L. Weiwen, "Research on improved rotor position detection method based on SMO," *J. Beijing Univ. Aeron. Astron.*, 1–15, 2019.
10. Liu, Y. C., S. Laghrouche, A. Nrdiaye, et al., "Active-flux-based super-twisting sliding mode observer for sensorless vector control of synchronous reluctance motor drives," *7th Int. IEEE Conf. Renew. Energy Res.*, Vol. 5, 402–406, 2018.
11. Chen, J., X. Wu, S. Chen, et al., "Sensorless flux adaption DTFC of an IPMSM based on an active fluxbased MTPA and an adaptive second-order sliding mode observer," *IET Power Electron.*, Vol. 13, No. 9, 1875–1884, 2020.
12. Li, W., Z. Du, W. Wang, et al., "Composite fractional order sliding mode control of permanent magnet synchronous motor based on disturbance observer," *2019 Chinese Automation Congress*, 4012–4016, 2019.
13. Huang, Y. and F. Wu, "A sensorless control method for permanent magnet synchronous motor based on fractional-order sliding mode observer," *2020 IEEE 5th Information Technology and Mechatronics Engineering Conference*, 1536–1542, 2020.
14. Nicola, M. and C. Nicola, "Sensorless control of PMSM using fractional order SMC and extended kalman observer," *2021 18th International Multi-Conference on Systems, Signals & Devices*, 526–532, 2021.
15. Jia, L., Y. Huang, J. Zheng, et al., "Fuzzy sliding mode control of permanent magnet synchronous motor based on the integral sliding mode surface," *2019 22nd International Conference on Electrical Machines and Systems*, 1–6, 2019.
16. Li, H. and Q. Wang, "Sliding mode controller based on fuzzy neural network optimization for direct torque controlled PMSM," *2010 8th World Congress on Intelligent Control and Automation*, 2434–2438, 2010.
17. Kuppusamy, S. and Y. H. Joo, "Memory-based integral sliding-mode control for T-S fuzzy systems with PMSM via disturbance observer," *IEEE Transactions on Cybernetics*, Vol. 51, No. 5, 2457–2465, 2021.
18. Murakami, M., S. Morimoto, Y. Inoue, et al., "Maximum torque per ampere control of an IPMSM with magnetic saturation using online parameter identification," *Proceedings of 2020 23rd International Conference on Electrical Machines and Systems*, 1631–1636, Hamamatsu, Japan, 2020.